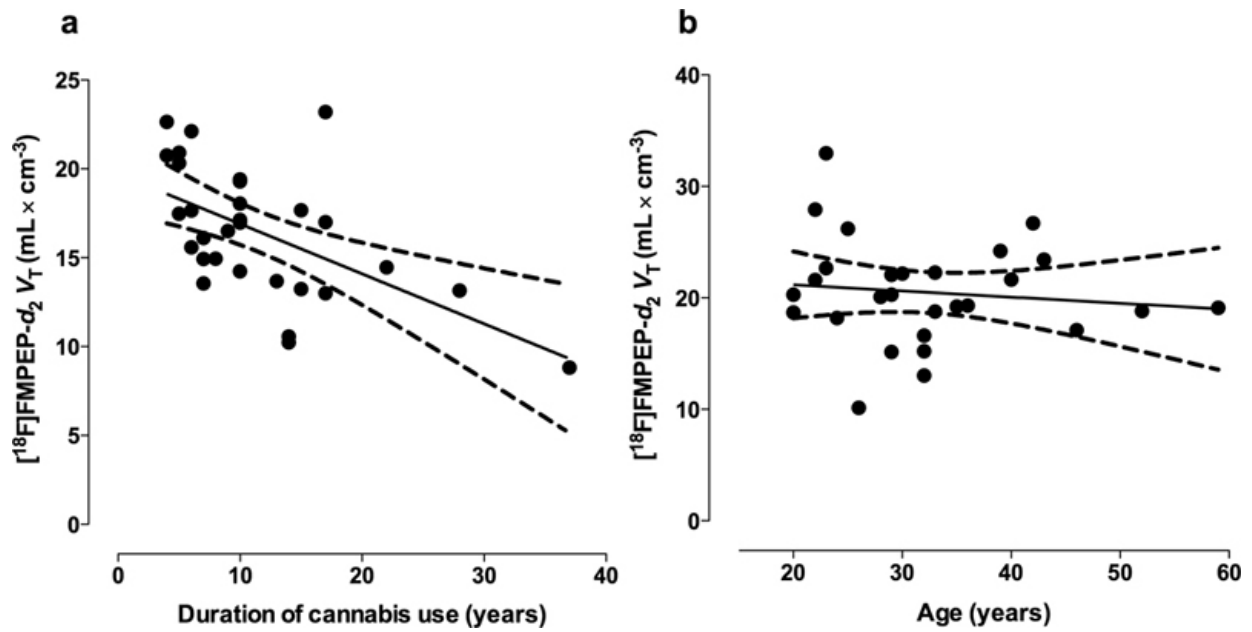
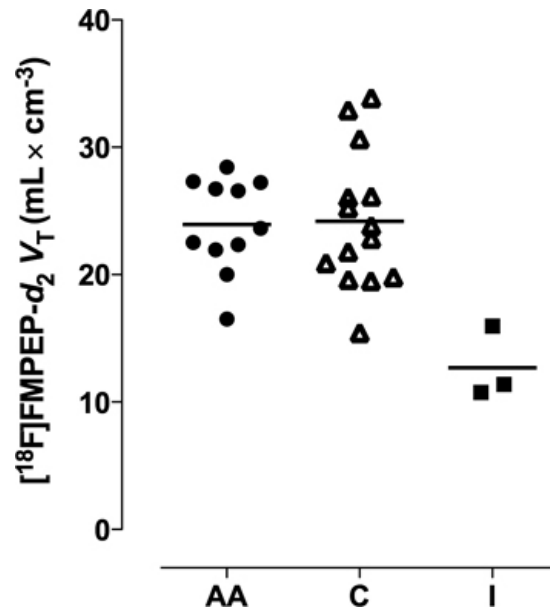


**Supplementary Figure 1.** BMI-adjusted  $V_T$  of [ $^{18}\text{F}$ ]FMPEP- $d_2$  at baseline in cannabis smokers (n=30) correlated negatively with years of cannabis smoking in prefrontal cortex ( $\rho=-0.55$ ,  $p=0.002$ ) (A). This correlation could be confounded by age. No correlation, however, was seen between BMI-adjusted  $V_T$  of [ $^{18}\text{F}$ ]FMPEP- $d_2$  and age in control subjects (n=28,  $R=-0.10$ ,  $p=0.615$ ) (B). Prefrontal cortex is representative of all neocortical regions. Curved dashed lines are bounds for the 95% confident interval for a linear regression fit for visualization purposes.



**Supplementary Figure 2.** Control subjects of Indian descent had lower BMI-adjusted  $V_T$  of  $[^{18}\text{F}]\text{FMPEP-}d_2$  in prefrontal cortex than other control subjects. Prefrontal cortex is representative of all brain regions. AA, African-American; C, Caucasian of European descent; I, Indian.



## Supplementary Methods

### *Positron emission tomography*

PET images were spatially normalized to a ligand-specific template using Statistical Parametric Mapping package (SPM5)<sup>1</sup> running on Matlab (version 7.2.0.232, Mathworks, Natick, MA) by estimating parameters from time-averaged PET images. The ligand-specific template was created in-house using PET images from twelve healthy subjects. Regional radioactivity concentration was measured from the spatially normalized dynamic PET images and the Automated Anatomical Labeling template of volumes of interest<sup>2</sup> as implemented in PMOD, version 3.0 (PMOD Technologies Ltd)<sup>3</sup>. Data from the Automated Anatomical Labeling template were consolidated by volume-weighted averaging into the following volumes of interest: anterior cingulate cortex, amygdala, caudate, cerebellum, hippocampus, insula, occipital cortex, parietal cortex, posterior cingulate cortex, parahippocampal gyrus, putamen, lateral temporal cortex, and thalamus. The following volumes of interest were manually added to the template: midbrain, pons, ventral striatum, and white matter. Ventral striatum was delineated onto coronal sections according to a published guideline<sup>4</sup>. Distribution volume ( $V_T$ ) was estimated according to the 2-tissue compartmental model<sup>5</sup> with concentration of parent radioligand in plasma as input function, using PMOD, as previously described<sup>6</sup>.

### *Voxel-wise analysis of $V_T$*

To confirm results from volume of interest analysis and to explore regional specificity of findings, we compared baseline parametric  $V_T$  maps between groups at voxel-level using SPM5. Parametric  $V_T$  images were calculated using the Logan plot with arterial input function as implemented in PMOD.  $V_T$  images were then smoothed

with a 12-mm Gaussian kernel (full width at half maximum), and tested between groups at baseline using a two-sample t-test with BMI as covariate in SPM5. No global normalization was applied. Cluster-level corrected p-values smaller than 0.05 were considered statistically significant.

## References

1. Friston, K.J., Holmes, A.P., Worsley, K.J., Poline, J.P., Frith, C. & Frackowiak, R.S.J. Statistical parametric maps in functional imaging: a general linear approach. *Human Brain Mapping* 1995; **2**, 189-210.
2. Tzourio-Mazoyer, N., Landeau, B., Papathanassiou, D., Crivello, F., Etard, O., Delcroix, N. *et al.* Automated anatomical labeling of activations in SPM using a macroscopic anatomical parcellation of the MNI MRI single-subject brain. *Neuroimage* 2002; **15**, 273-289.
3. Burger, C., Mikołajczyk, K., Grodzki, M., Rudnicki, P., Szabatin, M. & Buck, A. Java tools for quantitative post-processing of brain PET data. *Journal of Nuclear Medicine* 1998; **39**, 277p-278p.
4. Mawlawi, O., Martinez, D., Slifstein, M., Broft, A., Chatterjee, R., Hwang, D.R. *et al.* Imaging human mesolimbic dopamine transmission with positron emission tomography: I. Accuracy and precision of D(2) receptor parameter measurements in ventral striatum. *J Cereb Blood Flow Metab* 2001; **21**, 1034-1057.
5. Innis, R.B., Cunningham, V.J., Delforge, J., Fujita, M., Gjedde, A., Gunn, R.N. *et al.* Consensus nomenclature for in vivo imaging of reversibly binding radioligands. *J Cereb Blood Flow Metab* 2007; **27**, 1533-1539.

6. Terry, G.E., Hirvonen, J., Liow, J.S., Zoghbi, S.S., Gladding, R., Tauscher, J.T. *et al.* Imaging and quantitation of cannabinoid CB1 receptors in human and monkey brains using (18)F-labeled inverse agonist radioligands. *J Nucl Med* 2010; **51**, 112-120.